3.10 *Electron density of states inside quantum wires.* The electron energy dispersion in an infinite potential barrier quantum wire can be expressed as

$$E(k_x, \ell, n) = \frac{\hbar^2 k_x^2}{2m^*} + \frac{\hbar^2 \pi^2}{2m^*}\left[\left(\frac{\ell}{L_y}\right)^2 + \left(\frac{n}{L_z}\right)^2\right]$$

where ℓ, n can take integer values $1, 2, \ldots$. Derive an expression for the electron density of states and plot this expression for $L_y = L_z = 50$ Å.

3.11 *Electron density of states inside quantum dots.* Determine the electron density of states of a cubic quantum dot with side length $d = 20$ Å, assuming that the electron effective mass equals the free electron mass.

3.12 *Phonon density of states.* Assuming that phonons of a three-dimensional crystal obey the following isotropic dispersion relation,

$$\omega = 2\sqrt{\frac{K}{m}}\left|\sin\frac{ka}{2}\right|$$

where a is the lattice constant, derive an expression for the phonon density of states.

3.13 *Debye approximation.* Derive an expression for sound velocity from eq. (3.45). Calculate the sound velocity for a monatomic fcc crystal along (100) and (111) directions, using this simplified expression. Assume that the mass of the atom is 9.32×10^{-23} kg, the lattice constant of the conventional fcc unit cell is 5.54×10^{-10} m, and the spring constant is 7600 N m^{-1}.

3.14 *Transverse and longitudinal phonons.* Consider three separate acoustic phonons in a three-dimensional isotropic medium with an effective lattice constant of 2.5 Å. The dispersion for each branch is $\omega_L = v_L k$, $\omega_t = v_t k$ (degenerate). For $v_L = 8000$ m s^{-1} and $v_t = 5000$ m s^{-1}, plot the density of states as a function of frequency.

3.15 *Size effects on density of states.* The density of states expressions we derived are valid when the separations between states are small and the number of states is large, such that we can calculate the number of states by eq. (3.50). In small geometries, the energy separations between different states can be large and the number of states at each energy level can be small, so that eq. (3.50) is no longer valid. As an example, consider a cubic cavity of $(2\ \mu\text{m})^3$ size. Find out how many states are allowed to exist inside the cavity for electromagnetic waves with a wavelength in the range of 0.5–1 μm, using the following two methods:

(a) by finding out how many sets of (k_x, k_y, k_z) are allowed in this cavity that fall into the given wavelength range;

(b) by integrating eq. (3.59) over the given wavelength range.

4

Statistical Thermodynamics and Thermal Energy Storage

The quantum mechanics principles covered in the previous two chapters give the allowable energy states of matter. The number of allowable states in typical macroscopic matter is usually very large, and at any instant, the matter can be at any one of these states. Although our mathematical treatments in the previous two chapters were based on solving the steady-state Schrödinger equation for the energy states and the wavefunctions, matter will not stay at one particular quantum state (a microscopic state) for long because of the interactions among particles (atoms, molecules, electrons, and phonons) in the matter. For example, we assumed a harmonic potential between atoms to obtain the phonon dispersion relation. In reality, the interatomic potential is not harmonic, as one can easily infer from examining the Lennard–Jones potential. When the anharmonicity (the deviation from the harmonic potential) is small, the solutions of the Schrödinger equation for the quantum states based on the harmonic potential are approximately correct. Yet a small degree of anharmonicity can cause a rapid ($\sim 10^{-9}$–10^{-13} s) change of the matter from one quantum state to another. Due to the large number of quantum states available in matter, it is impractical to follow the real time evolution of matter among its allowable quantum states. The bridge connecting the allowable quantum states to the macroscopic behavior is provided by statistical thermodynamics, which determines the probability that matter will be at a particular quantum state when it is at equilibrium. Through statistical thermodynamics, temperature enters into the picture of energy storage and transport.

In this chapter, we focus on the equilibrium state of a system and discuss different probability functions for systems under different constraints, such as an isolated system or a system at constant temperature. From the probability distribution functions, we will show how to calculate the internal energy and specific heat of a system, including

nanostructures, using what we learned in previous chapters about the energy levels, degeneracy, and the density of states.

4.1 Ensembles and Statistical Distribution Functions

In an actual experiment, we often follow the time history of a system and observe its time-averaged behavior. In analysis, however, following the time history requires the solution of master equations that govern the motion of a large number of particles, such as the Newton equations of motion and the time-dependent Schrödinger equation. Although, with increasing computational power, such computation is becoming feasible for limited situations, as in the molecular dynamics simulations to be introduced in chapter 10, for most applications direct computation of the time history is impractical. Statistical thermodynamics avoids the time averaging by introducing *ensembles*, which are large collections of systems, each representing a microscopic state that satisfies the macroscopic constraints. Examples of the macroscopic constraints of a system are its total energy, temperature, and volume. The quantities to be measured are averaged over the ensemble at a fixed time, rather than, as in an experimental situation, over a time period of a single system. A fundamental assumption made in statistical mechanics is that the ensemble average of an observed quantity is equal to the time average of the same quantity. This assumption is called the *ergodic hypothesis*. The study of conditions necessary for this hypothesis to be valid is an ongoing research area (Kubo et al., 1998). Our analysis will assume that all systems are ergodic. Depending on the macroscopic constraints, various ensembles are developed, each has a probability distribution for the microscopic states in the ensemble that differs from other ensembles. In the following, we will discuss three ensembles: microcanonical, canonical, and grand canonical ensembles.

4.1.1 Microcanonical Ensemble and Entropy

Unlike classical thermodynamics, which completely neglects the microscopic processes in a system, statistical thermodynamics builds the system properties from its microscopic states (Kittel and Kroemer, 1980; Callen, 1985). We consider an *isolated* macroscopic system with a volume V, a total number of particles N, and a total energy of U (macroscopic constraints). The quantum states of the system that satisfy these macroscopic constraints are called the accessible quantum states (or simply accessible states). Given these macroscopic constraints, together with detailed information about the interatomic potentials between the particles in the system and the initial conditions, one could in principle solve the Schrödinger equation to follow the temporal evolution of the system among the accessible quantum states. The macroscopic properties of the system, such as temperature and pressure, are a measure of the average corresponding microscopic properties over a certain amount of time.

How can we calculate the average values of this system? If we performed an experiment, we would measure these values as a function of time and carry out a time average. In statistical mechanics, instead of tracing the time evolution of the system, we focus on the probability of a system being at a specific accessible quantum state. A *fundamental*

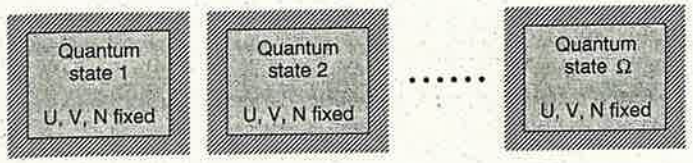

Figure 4.1 A microcanonical ensemble is made of isolated systems with fixed U, V, and N. Each system corresponds to one accessible quantum state of the original system.

postulate in statistical mechanics is that an isolated macroscopic system samples every accessible quantum state with equal probability. This postulate is also called the *principle of equal probability*. If Ω is the total number of accessible quantum states, the probability of each accessible quantum state, denoted by s, being sampled is

$$P(s) = 1/\Omega \tag{4.1}$$

Once the probability of each accessible quantum state is known, we can construct a way to calculate a desired macroscopic quantity $\langle X \rangle$ of a macroscopic system. We first evaluate the corresponding property X (such as temperature, pressure) for each accessible quantum state, and then calculate the average according to

$$\langle X \rangle = \sum_{s=1}^{\Omega} P(s)X(s) \tag{4.2}$$

Note that the summation is over all accessible quantum states.

Because each accessible quantum state is a state of the system that satisfies the macroscopic constraints and each one has equal probability to be sampled, we are effectively dealing with a collection of Ω stationary systems, as shown in figure 4.1. These systems are identical from the macroscopic points of view; that is, they have the same U, V, and N and are all isolated from their surroundings. This collection of Ω systems is called an *ensemble*. A fixed U, V, N ensemble is called a *microcanonical* ensemble. The principle of equal probability is valid only for each system in a microcanonical ensemble. Later, we will introduce canonical and grand canonical ensembles and derive the probability of each system in such ensembles on the basis of results we obtained from the microcanonical ensemble. Equation (4.2) means that each of the stationary systems in the ensemble is sampled once in the computing of the average. Such an average is called the ensemble average. For a microcanonical ensemble, $P(s) = 1/\Omega$, thus

$$\langle X \rangle = \sum_{s=1}^{\Omega} X(s)/\Omega \tag{4.3}$$

The idea of equal probability for each accessible quantum state in an isolated system may seem unreasonable for some readers. For example, for a system of 10^{23} particles, one accessible quantum state might be that one particle has energy U and the rest have zero energy. This distribution of energy among N particles seems to be a quite unlikely

event but the principle of equal probability states that such a state is just as probable as any other quantum states, for example, a state in which each particle has an energy U/N (assuming that such a state is also accessible). The latter is perceived to be more likely. This concern can be resolved by noting that there is usually a large number of accessible states close to the latter case (large degeneracy) so that an actual observation would most likely sample one of these high-degeneracy states.

Suppose that we have determined the number of accessible states Ω of an isolated system with fixed U, V, and N. How can we relate Ω to macroscopic thermodynamic quantities? For a microcanonical ensemble, we rarely use eq. (4.3) to calculate the average quantities. Rather, we use a crucial link established by Ludwig Boltzmann (1844–1906), who showed that Ω is directly related to the entropy of the system through

$$S = \kappa_B \ln \Omega \tag{4.4}$$

where κ_B is the Boltzmann constant ($= 1.38 \times 10^{-23}\,\mathrm{J\,K^{-1}}$). Equation (4.4) is called the *Boltzmann principle*. This relation between entropy and accessible states is consistent with the typical interpretation in classical thermodynamics that entropy is a measure of the randomness of the system. The larger the number of accessible states, the more freedom a macroscopic system has, and thus the more randomness it has. The Boltzmann constant (and its units) is a conversion factor that makes the classical definition of entropy consistent with its microscopic definition while the logarithm satisfies the additiveness of the entropy used in classical thermodynamics. For example, if the system can be divided into two subsystems, each having Ω_1 and Ω_2 accessible states, the total number of accessible states of the system is then $\Omega_1 \times \Omega_2$. Equation (4.4) leads to $S = S_1 + S_2$, satisfying the additiveness of entropy.

Because Ω is constrained by U, V, and N, we anticipate that it is a function of these variables, and thus so is entropy,

$$S = S(U, V, N) \tag{4.5}$$

If we know the above function, we can construct all other thermodynamic properties of the system. For example, eq. (4.5) can be written as

$$dS = \left(\frac{\partial S}{\partial U}\right)_{V,N} dU + \left(\frac{\partial S}{\partial V}\right)_{U,N} dV + \left(\frac{\partial S}{\partial N}\right)_{U,V} dN$$

The above equation, when combined with the more familiar form of $dU = T\,dS - p\,dV + \mu\,dN$ from classical thermodynamics, immediately leads to

$$\frac{1}{T} = \left(\frac{\partial S}{\partial U}\right)_{V,N}, \frac{p}{T} = \left(\frac{\partial S}{\partial V}\right)_{U,N}, -\frac{\mu}{T} = \left(\frac{\partial S}{\partial N}\right)_{U,V} \tag{4.6}$$

where μ is the chemical potential. Equation (4.6) means that if we know the function $S(U,V,N)$ [or $U(S,V,N)$], we can determine all other thermodynamic state variables such as temperature, pressure, and chemical potential. The function $S(U,V,N)$ is called a *thermodynamic potential*.

It is important to realize that a thermodynamic potential must be expressed in terms of its corresponding variables U, V, and N. Not any arbitrary combination of macroscopic thermodynamic properties can be the variables of a thermodynamic potential. For example, a known function of entropy $S(T, p, N)$ with T, p, N as variables does not give all the other thermodynamic properties of the system and is thus not a thermodynamic potential. In the next section, we will examine two other types of ensemble, each leads to the construction of a thermodynamic potential that gives a full description of the macroscopic thermodynamic properties of the system.

4.1.2 Canonical and Grand Canonical Ensembles

In practice, we are often more interested in determining how system properties change with temperature. The microcanonical ensemble is not convenient for this purpose since one of its natural thermodynamic variables is internal energy rather than temperature. Instead of considering an isolated system of fixed energy, let's now consider a system of given temperature T, fixed volume V, and fixed number of particles N. To maintain the system at a fixed temperature, we assume that it is in contact with a thermal reservoir at the same temperature. A thermal reservoir is a very large object, such that its temperature does not change even if there is energy transfer between the system and the reservoir. Because of this energy exchange, the system energy is not fixed. Our goal is to obtain the probability of finding the system at a specific accessible quantum state with energy E_i, satisfying the macroscopic constraints of constant T, V, and N. We will see that, because of the change of constraint from fixed U to fixed T, the probability of observing each accessible quantum state is no longer identical as in a microcanonical ensemble.

We start from the microcanonical ensemble statistics established in the previous section by considering that the system (and let's call it the original system) and the thermal reservoir form a large isolated system (we will call it the combined system) with fixed U_t, V_t, and N_t. The combined system has a total number of Ω_t quantum states. We can construct a microcanonical ensemble of the combined system as shown in figure 4.2. In such an ensemble, because the reservoir is very large, the total number of accessible quantum states of the combined system Ω_t is much larger than the number of accessible quantum states Ω_s of the original system. It is very likely that corresponding to a specific accessible quantum state of the original system there are many accessible quantum states in the reservoir. Rather than examining a microcanonical ensemble of the combined system as shown in figure 4.2(a), we construct a new ensemble made of Ω_s systems. Each of the systems in the new ensemble is an accessible quantum state of the original system with macroscopic constraints of constant T, V, and N, as shown in figure 4.2(b), and is in thermal equilibrium with a common reservoir. Because each system in the new ensemble may have a different number of accessible states in the reservoir, the chance that we observe each system in the ensemble is no longer identical to each other as in a microcanonical ensemble. Consequently, we call this ensemble a *canonical ensemble*. We would like to determine the probability of finding a system at a specific accessible quantum state with an energy E_i. Let's assume that there are $\Omega_r(U_t - E_i)$ accessible states in the reservoir corresponding to this specific system state. The probability of observing the system is then

$$P(E_i) = \frac{\Omega_r(U_t - E_i)}{\Omega_t(E_t)} \tag{4.7}$$

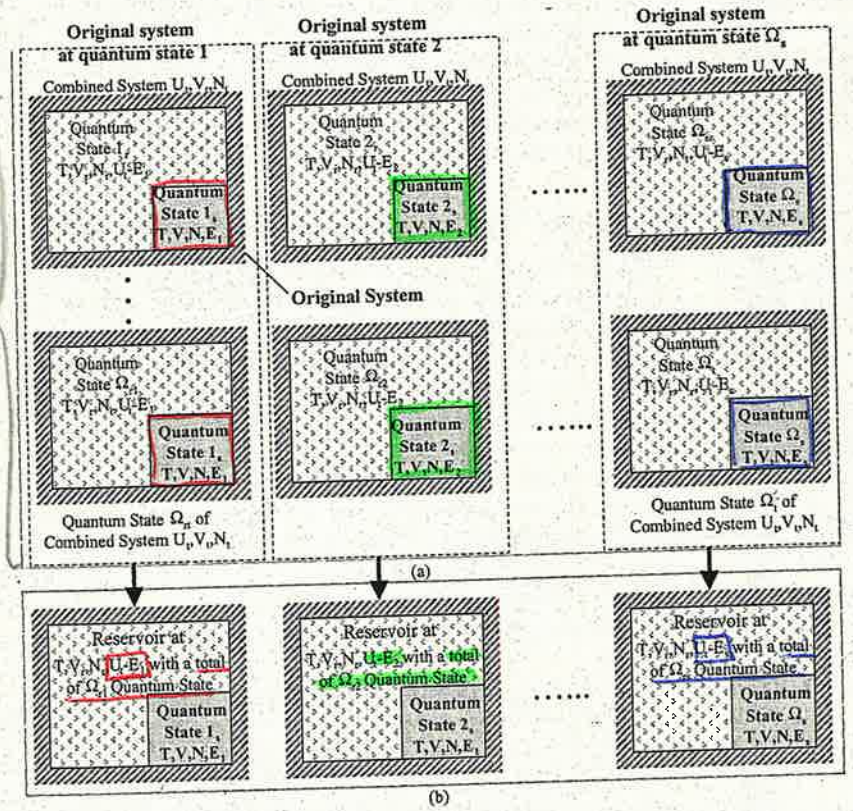

Figure 4.2 Constructing a canonical ensemble from a microcanonical ensemble. (a) A microcanonical ensemble for the combined system comprises the reservoir and the original system, with a total of Ω_t systems, each with equal probability. Each column represents microcanonical ensembles with the original system in one quantum state, while the reservoirs may have many quantum states. (b) A canonical ensemble has Ω_s systems with fixed T, V, and N. Each system has a number of quantum states in the reservoir and thus not every system has an equal probability of being observed.

To find Ω_r in the above expression, we consider another combined system made of one quantum state of the original system at energy E_i and Ω_r quantum states of the reservoir with an energy $(U_t - E_i)$. This "new" combined system occupies only one column in figure 4.2(a) of the previously established "old" combined microcanonical ensemble and is also a microcanonical ensemble because of its fixed energy. Assuming that the entropy of this new combined system is S_r and the entropy of the old microcanonical ensemble in figure 4.2(a) is $S_t(U_t)$, we can use eq. (4.4) to rewrite eq. (4.7) as

$$P(E_i) = \frac{\exp\left[S_r(U_t - E_i)/\kappa_B\right]}{\exp\left[S_t(U_t)/\kappa_B\right]} \tag{4.8}$$

If U is the average energy of the original system, then the total entropy of the old combined system is

$$S_t(U_t) = S_r(U_t - U) + S(U) \tag{4.9}$$

By a Taylor expansion, we can express $S_r(U_t - E_i)$ as

$$\begin{aligned} S_r(U_t - E_i) &= S_r[(U_t - U) + (U - E_i)] \\ &= S_r(U_t - U) + \left.\frac{\partial S_r}{\partial E_r}\right|_{U_t - U}(U - E_i) \\ &= S_r(U_t - U) + \frac{U - E_i}{T} \end{aligned} \tag{4.10}$$

where we have applied eq. (4.6) to the new combined microcanonical ensemble,

$$\frac{1}{T} = \left[\frac{\partial S_r}{\partial E_r}\right]_{U_t - U} \tag{4.11}$$

Substituting eq. (4.10) into eq. (4.8) leads to

$$P(E_i) = \exp\left[\frac{U - TS}{\kappa_B T}\right]\exp\left[-\frac{E_i}{\kappa_B T}\right] \tag{4.12}$$

where we have used $S(U) = S_t(U_t) - S_r(U_t - U)$, that is, eq. (4.9), to eliminate the entropy of the thermal reservoir. We recognize that $F = U - TS$ is the *Helmholtz free energy* of the system—a thermodynamic potential with natural variables of T, V, and N. Given $F(T, V, N)$, we can calculate all other thermodynamic properties of the system. We use the probability normalization requirement to find F,

$$\sum_i P(E_i) = \exp\left[\frac{F}{\kappa_B T}\right]\sum_i \exp\left[-\frac{E_i}{\kappa_B T}\right] = 1 \tag{4.13}$$

where the summation is over all the accessible quantum states of the system. Equation (4.13) gives

$$F(T, V, N) = -\kappa_B T \ln Z \tag{4.14}$$

where Z is called the *canonical partition function*

$$Z = \sum_i \exp\left[-\frac{E_i}{\kappa_B T}\right] \tag{4.15}$$

Substituting eq. (4.14) into eq. (4.12) leads to the probability of a fixed V, N, T system at a quantum state having energy E_i as

$$P(E_i) = e^{-E_i/k_B T}/Z \tag{4.16}$$

The factor $\exp(-E_i/k_B T)$ is called the *Boltzmann factor*. It is widely seen in different disciplines of science. You may have encountered this exponential form somewhere else.

For example, the Arrhenius law governing chemical reactions is a manifestation of the Boltzmann factor.

A similar analysis can be extended to consider a system of fixed volume that exchanges both energy and particles with a larger reservoir. From classical thermodynamics, we know that the driving force for particle flow is the chemical potential that is defined by eq. (4.6). An ensemble of such a system in equilibrium with the reservoir is called a *grand canonical ensemble*. The variables for such an ensemble are T, V, and μ, and the corresponding thermodynamic potential is called the *grand canonical potential* $G(T, V, \mu)$. Following a similar analysis to that of a canonical ensemble, the probability of a quantum state having energy E_i and number of particles N_i is given by

$$P(E_i, N_i) = \frac{\exp\left[\frac{N_i\mu - E_i}{\kappa_B T}\right]}{\Im} \tag{4.17}$$

The exponential factor is called the *Gibbs factor* and the denominator is the *grand canonical partition function*, given by

$$\Im(T, V, \mu) = \sum_{N_i}\sum_{E_i} \exp\left[\frac{N_i\mu - E_i}{\kappa_B T}\right] = \sum_{N_i} \gamma^{N_i} Z_i \tag{4.18}$$

where $\gamma = \exp(\mu/\kappa_B T)$ and the double summation is over all accessible energy states and number of the particles of the system. The grand canonical potential is

$$G(T, V, \mu) = U - TS - \mu N = -\kappa_B T \ln \Im \tag{4.19}$$

where U and N are the average energy and number of particles of the system, respectively.

4.1.3 Molecular Partition Functions

The above discussion shows that if the partition function is known, the thermodynamic potential of a system can be determined, and consequently all other thermodynamic quantities are also known. We discuss below the partition function of gas molecules.

Let's start with the partition function of a single molecule. To find the accessible quantum states, we can extend the solution for the energy levels of a particle-in-a-potential-well model to the three-dimensional case and arrive at the following form of the quantized energy levels for the translational motion of a gas molecule in a cubic box of length L [see eq. (E2.1.6)],

$$E = \frac{\pi^2\hbar^2}{2mL^2}(n_x^2 + n_y^2 + n_z^2) \text{ where } n_x, n_y, n_z = 1, 2, 3, \ldots \tag{4.20}$$

and the density of states per unit volume is

$$D(E) = \frac{1}{4\pi^2}(2m/\hbar^2)^{3/2} E^{1/2} \tag{4.21}$$

Substituting eq. (4.20) into eq. (4.15) leads to the canonical partition function for the translational motion of one gas molecule,

$$Z = \sum_{n_x=1}^{\infty}\sum_{n_y=1}^{\infty}\sum_{n_z=1}^{\infty} \exp\left[-\frac{\pi^2\hbar^2(n_x^2 + n_y^2 + n_z^2)}{2mL^2\kappa_B T}\right] \tag{4.22}$$

To evaluate the above triple summation, we first notice that $\lfloor \pi^2\hbar^2/(2mL^2\kappa_B T)\rfloor$ in the exponent is a very small number such that the exponential function is slowly varying. Second, n_x, n_y, and n_z are integers spaced by Δn_x (or Δn_y, Δn_z) $= 1$. Due to the above two reasons, the summation can be well approximated by integration,

$$Z = \int_0^{\infty}\int_0^{\infty}\int_0^{\infty} \exp\left[-\frac{\pi^2\hbar^2(n_x^2 + n_y^2 + n_z^2)}{2mL^2\kappa_B T}\right] dn_x dn_y dn_z$$

$$= V\left(\frac{2\pi m\kappa_B T}{h^2}\right)^{3/2} = \frac{V}{\lambda^3} \tag{4.23}$$

where $V = L^3$ and

$$\lambda = \frac{h}{\sqrt{2\pi m\kappa_B T}} \tag{4.24}$$

is called the *thermal de Broglie wavelength*.

Another way to arrive at the same answer as eq. (4.23) is to realize that the triple summation in eq. (4.22) is essentially sampling all the quantum states. With a slowly varying exponential, we can convert this summation over the quantum states into an integration over allowable energy levels, using the density-of-states,

$$Z = V\int_0^{\infty} \exp\left[-\frac{E}{\kappa_B T}\right] D(E)dE$$

$$= V\int_0^{\infty} \frac{1}{4\pi^2}\left(\frac{2m}{\hbar^2}\right)^{3/2} E^{1/2} \exp\left[-\frac{E}{\kappa_B T}\right] dE = \frac{V}{\lambda^3} \tag{4.25}$$

which is identical to eq. (4.23).

For a dilute gaseous system with N molecules, the energy eigenvalues from a single particle-in-a-box model apply to every particle because the potential interactions among the particles are weak. The total energy of the system equals the summation of the energy of all particles $E_t = E_1 + E_2 + \cdots + E_N$, where E_i represents the possible energy values of particle i and is given by eq. (4.20) without any additional constraints for the indices n_{xi}, n_{yi}, n_{zi}, because the total energy of a canonical system is not a prior constraint of the system and thus can take any value. From eq. (4.15), we can write the canonical particle function for this N-molecule system as

$$Z_N = \sum_{n_{x1}, n_{y1}, n_{z1}} \sum_{n_{x2}, n_{y2}, n_{z2}} \cdots \sum_{n_{xN}, n_{yN}, n_{zN}} \exp\left(-\frac{E_1 + E_2 + \cdots + E_N}{\kappa_B T}\right) \tag{4.26}$$

where each summation is over all possible states of molecule i as determined by indices (n_{xi}, n_{yi}, n_{zi}) with specified values as in eq. (4.22). If the molecules were distinguishable, that is, if every quantum state of particle i were different from that of particle j, eq. (4.22) could be factorized into Z^N. Real molecules, however, are identical to each other and are thus indistinguishable. This indinstinguishability affects how we perform the summations in eq. (4.26) because one accessible quantum state should be counted only once in the summation. The indistinguishability of molecules means that if two molecules i and j are at an identical quantum state, for example, with $n_{xi} = n_{xj} = 10, n_{yi} = n_{yj} = 10$, and $n_{zi} = n_{zj} = 10$, they should be counted in the summation of eq. (4.26) once only rather than twice because no way exists to distinguish the two molecules in the system. In general, counting such indistinguishable cases is difficult, but can be done when the accessible quantum states of one molecule as given by eq. (4.20) are much larger than the total number of molecules such that no two molecules occupy the same energy states at the same time. Under this dilute-gas limit, we overcount the indistinguishable molecules by $N!$ when treating them as distinguishable, where $N! = N(N-1)(N-2)\ldots 1$ is the factorial of N. Thus in the dilute gas limit, the canonical partition function, eq. (4.26), can be simplified to

$$Z_N \approx \frac{Z^N}{N!} = \frac{1}{N!}\left(\frac{V}{\lambda^3}\right)^N \tag{4.27}$$

From the canonical partition function Z_N, we can calculate the Helmholtz energy of the gas system:

$$F(T,V,N) = -\kappa_B T \ln Z_N = -N\kappa_B T\left[\ln V - \frac{3}{2}\ln\left(\frac{h^2}{2\pi m \kappa_B T}\right)\right] + \kappa_B T(N\ln N - N) \tag{4.28}$$

where we have used the Stirling approximation: $\ln N! \approx N\ln N - N$. This approximation is valid when N is large, which is typically the case. With $F(T, V, N)$ known, all other thermodynamic quantities of the system can be obtained. For example, from $dF = -S\,dT - p\,dV + \mu\,dN$, we can calculate the pressure as

$$p = -\left(\frac{\partial F}{\partial V}\right)_{T,N} = \frac{\kappa_B T N}{V} \tag{4.29}$$

and the internal energy can be calculated from

$$U = \sum_i E_i P(E_i) = \sum_i \frac{E_i \exp(-E_i/\kappa_B T)}{Z_N} = \kappa_B T^2 \frac{\partial \ln Z_N}{\partial T} = \frac{3N\kappa_B T}{2} \tag{4.30}$$

The last two equations should be familiar. Equation (4.29) is the ideal gas law that applies to dilute gas. Equation (4.30) is equivalent to eq. (1.28) and is a special case of the *equipartition theorem*, which says that, at high temperature, every degree of freedom with a quadratic energy term contributes $\kappa_B T/2$ to the average energy of the system.

A monatomic molecule has three degrees of translational freedom only and the energy is in quadratic form, as eq. (4.20) shows. Each quadratic term in energy contributes $\kappa_B T/2$, and thus, we have an average energy of $3\kappa_B T/2$ for each molecule.

For a polyatomic gas, the energy level of each molecule can be separated into translational, vibrational, rotational, and electronic components:

$$E = E_t + E_v + E_r + E_e \tag{4.31}$$

and the corresponding partition function is

$$Z = \sum e^{-E/\kappa_B T} = \sum e^{-E_t/\kappa_B T}\sum e^{-E_v/\kappa_B T}\sum e^{-E_r/\kappa_B T}\sum e^{-E_e/\kappa_B T} = Z_t Z_v Z_r Z_e \tag{4.32}$$

where Z_t, Z_v, Z_r, and Z_e are the canonical partition functions for each energy component of the molecule as represented by the corresponding subscripts. Once the partition function for one molecule is known, the canonical partition function for a dilute system of N molecules can be calculated from eq. (4.27).

Before concluding this section, we present a criterion that determines when the dilute gas limit, which leads to the factorial $N!$ in eq. (4.27), is valid. The requirement for this limit is that the number of quantum states for one molecule is much larger than the number of molecules in the box. Thus if the number of quantum states between zero energy and the average molecular energy is much larger than the number of molecules per unit volume, then the dilute gas assumption should be valid; in other words,

$$\int_0^{3\kappa_B T/2} D(E)dE \gg \frac{N}{V} \tag{4.33}$$

where the left-hand side is the number of quantum states with an energy between zero and $3\kappa_B T/2$. Substituting eq. (4.21) into eq. (4.33) and carrying out the integration, we obtain a criterion for the dilute gas assumption to be valid as

$$\frac{6N}{\pi V}\left(\frac{h^2}{12m\kappa_B T}\right)^{3/2} \ll 1 \text{ or } \frac{N}{V}\left(\frac{\pi}{6}\right)^{1/2}\lambda^3 \ll 1 \tag{4.34}$$

Because the intermolecular distance is of the order of $(V/N)^{1/3}$, eq. (4.34) also means that the thermal de Broglie wavelength must be much smaller than the intermolecular distance.

Example 4.1 *Canonical partition function*

Derive an expression for the canonical partition function of the rotational modes of a H_2 molecule in a box of H_2 gas.

Solution: We have obtained in chapter 2 the energy, eq. (2.65), and degeneracy, eq. (2.66), of a rigid rotor as

$$E_\ell = \frac{\hbar^2}{2I}\ell(\ell+1) = B\ell(\ell+1)(\ell = 0, 1, 2, \ldots, |m| \le \ell) \tag{E4.1.1}$$

$$g(\ell) = 2\ell + 1 \tag{E4.1.2}$$

where ℓ and m are the two quantum numbers of rational wavefunctions, and B is the rotational constant. The canonical partition function for the rotational modes is

$$Z_r = \sum_{\ell,m} \exp\left(-\frac{E_\ell}{\kappa_B T}\right) = \sum_{\ell=0}^{\infty} g(\ell)\exp\left(-\frac{E_\ell}{\kappa_B T}\right)$$
$$= \int_0^\infty (2\ell+1)\exp\left[-\frac{B\ell(\ell+1)}{\kappa_B T}\right]d\ell = \frac{8\pi^2 I\kappa_B T}{h^2} = \frac{T}{\theta_r} \tag{E4.1.3}$$

where θ_r is called the rotational temperature

$$\theta_r = \frac{hB}{\kappa_B} = \frac{h^2}{8\pi^2\kappa_B I} \tag{E4.1.4}$$

In eq. (E.4.1.3), the first summation over all ℓ and m is over all quantum states and the second summation over ℓ is over all energy levels. Similarly to eq. (4.23), we have converted the summation into an integral.

Comments. For hydrogen, $B = 1.8 \times 10^{12}$ Hz and $\theta_r = 85.3$ K. The transformation in eq. (E.4.1.3) from the summation into the integral is valid only when T is much larger than θ_r, that is, when changing ℓ by 1 does not change the exponential rapidly. So eq. (E4.1.4) is valid only for $T \gg \theta_r$. In the limit, when T is comparable to θ_r or smaller, we can take the first few terms of the summation to get

$$Z_r = 1 + 3\exp\left(-\frac{3\theta_r}{T}\right) + \cdots \tag{E4.1.5}$$

4.1.4 Fermi–Dirac, Bose–Einstein, and Boltzmann Distributions

Let's now consider the probability of electrons occupying a specific quantum state. We assume that we have determined the accessible quantum states for electrons in a given system. From the Pauli exclusion principle, each quantum state can have a maximum of one electron. If the system is at equilibrium with a temperature T, we wish to determine the probability of one quantum state having energy E being empty or occupied by one electron. We take this specific quantum state as our system, and the rest of the accessible quantum states of the original system are grouped into the reservoir. There can be energy and particle exchanges between the new system and its reservoir because an electron can fluctuate randomly between this quantum state and other quantum states. Thus the

appropriate ensemble for the new system is the grand canonical ensemble. The grand canonical partition function for the new system can be evaluated from eq. (4.18),

$$\Im(T, V, \mu) = \sum_{N_i=0}^{1} \gamma^{N_i} Z_i = 1 + \exp\left(\frac{\mu - E}{\kappa_B T}\right) \tag{4.35}$$

where $N_i = 0$ means that the quantum state is unoccupied, with system energy at zero, and $N_i = 1$ means that the state is occupied, with system energy at E. According to eq. (4.17), the probability that this quantum state is empty or occupied is, respectively,

$$P(E_i = 0, N_i = 0) = P_0 = \frac{1}{1 + \exp\left(\frac{\mu - E}{\kappa_B T}\right)} \quad \text{(empty)} \tag{4.36}$$

and

$$P(E_i = E, N_i = 1) = P_1 = \frac{\exp\left(\frac{\mu - E}{\kappa_B T}\right)}{1 + \exp\left(\frac{\mu - E}{\kappa_B T}\right)} \quad \text{(occupied)} \tag{4.37}$$

The average number of occupancy of this quantum state is thus

$$\langle n \rangle \equiv f(E) = 0 \times P(E_i = 0, N_i = 0) + 1 \times P(E_i = E, N_i = 1)$$
$$= \frac{1}{\exp\left(\frac{E - \mu}{\kappa_B T}\right) + 1} \tag{4.38}$$

and the average energy of this quantum state is

$$\langle E \rangle = 0 \times P(E_i = 0, N_i = 0) + E \times P(E_i = E, N_i = 1)$$
$$= \frac{E}{\exp\left(\frac{E - \mu}{\kappa_B T}\right) + 1} = Ef(E) \tag{4.39}$$

$\langle n \rangle$, or in a more popular symbol f, is called the *Fermi–Dirac distribution function*. Electrons and other particles that obey the Fermi–Dirac distributions are called *fermions*. Figure 4.3 illustrates this distribution function. Recall that μ is the chemical potential. When the energy is a few times of $\kappa_B T$ smaller than the chemical potential, the distribution is close to one, indicating that most of the energy states below the chemical potential are occupied. When the energy is a few times of $\kappa_B T$ larger than the chemical potential, the distribution function is close to zero, indicating that most states above the chemical potential are empty. Because the motion of electrons means that there must be unoccupied states for the electrons to fill, only the electrons close to the chemical potential are active in carrying the charge. At zero temperature, the chemical potential equals the Fermi level. In some fields, however, particularly electrical engineering, the chemical potential and the Fermi level are used interchangeably.

Next, let's consider the probability of phonons or photons occupying an accessible quantum state of the system. Unlike electrons, the number of phonons or photons in a system is not conserved. Thus N is not a thermodynamic variable for the system,

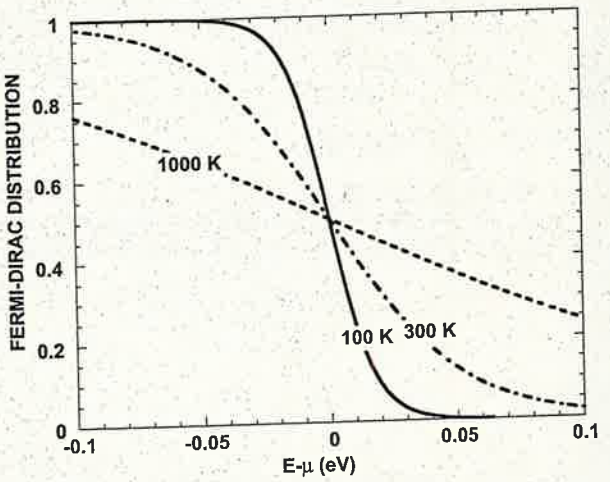

Figure 4.3 Fermi–Dirac distribution as a function of the electron energy relative to the chemical potential.

and, correspondingly, neither is the chemical potential. We know that for an accessible quantum state of the system, with frequency ν, there can be an arbitrary number n of photons or phonons such that the total energy of this state is $E = (n + 1/2)h\nu$ ($n = 0, 1, 2, \ldots$). Following a similar argument as for electrons, we take this quantum state to be our new system and the remaining quantum states to be the reservoir. Since neither the chemical potential nor the particle number is a thermodynamic variable, the new system is best described by a canonical ensemble with the canonical partition function

$$Z(\nu) = \sum_{n=0}^{\infty} \exp\left(-\frac{(n+1/2)\,h\nu}{\kappa_B T}\right) = \frac{\exp\left(-\frac{h\nu}{2\kappa_B T}\right)}{1 - \exp\left(-\frac{h\nu}{\kappa_B T}\right)} \tag{4.40}$$

The probability that the quantum state (the new system) has n particles (photons or phonons) is thus

$$P(\nu, n) = \frac{\exp\left(-\frac{(n+1/2)h\nu}{\kappa_B T}\right)}{Z} = \exp\left(-\frac{nh\nu}{\kappa_B T}\right)\left[1 - \exp\left(-\frac{h\nu}{\kappa_B T}\right)\right] \tag{4.41}$$

and the average number of the particles, or the occupancy of the quantum state, is

$$\langle n \rangle \equiv f(\nu) = \sum_{n=0}^{\infty} nP(\nu, n) = \frac{1}{\exp\left(\frac{h\nu}{\kappa_B T}\right) - 1} \tag{4.42}$$

This equation is the *Bose–Einstein distribution function*, and the particles obeying this distribution are called *bosons*. Figure 4.4 shows the Bose–Einstein distribution. Because each particle has energy $h\nu$, the average energy of the quantum state is

$$\langle E \rangle = h\nu f(\nu) \tag{4.43}$$

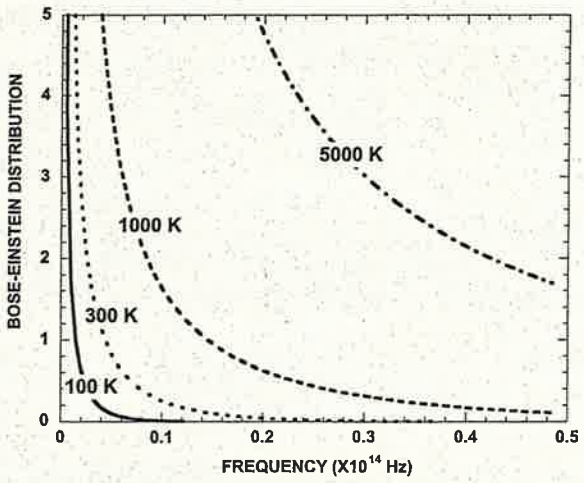

Figure 4.4 Bose–Einstein distribution as a function of the frequency of the carriers (phonons and photons).

where we have neglected the zero-point energy, which does not participate in heat transfer processes.

Other boson systems, such as gas molecules, can have a fixed number of particles. For such bosons, we should use the grand canonical ensemble as for fermions, and the general Bose–Einstein distribution can be written as

$$\langle n \rangle \equiv f(E) = \frac{1}{\exp\left(\frac{E-\mu}{\kappa_B T}\right) - 1} \tag{4.44}$$

where μ is again the chemical potential of the boson gas.

The Bose–Einstein distribution changes the "plus one" in the denominator of the Fermi–Dirac distribution into minus one. In the limit of low occupancy (high energy and high temperature), both Bose–Einstein and Fermi–Dirac distributions reduce to the Boltzmann distribution function

$$f(E, T, \mu) = \exp\left(-\frac{E-\mu}{\kappa_B T}\right) \text{ or } f(E) = \exp\left(-\frac{E}{\kappa_B T}\right) \tag{4.45}$$

This distribution function is considered as "classical", while the Fermi–Dirac and Bose–Einstein distributions are "quantum." Thus, for the statistical distributions, difference between "classical" and "quantum" statistics lies merely in the "one" of the denominator!

4.2 Internal Energy and Specific Heat

The statistical distribution functions establish a link with temperature between the quantum state and its energy level. With the distribution functions, we can investigate

the properties of matter at finite temperatures. In this section we consider the internal energy and specific heat. Recall that the constant volume specific heat per unit volume, C_V [J m^{-3} K^{-1}], is defined as

$$C_V = \frac{1}{V}\left(\frac{\partial U}{\partial T}\right)_V \tag{4.46}$$

where U is the average internal energy of the system. We will consider the internal energy and specific heat of various energy carriers in this section.

4.2.1 Gases

For a dilute monatomic gas, the total internal energy is given by eq. (4.30). Consequently, the volumetric specific heat is

$$C_V = \frac{1}{V}\frac{3}{2}\kappa_B N \tag{4.47}$$

Since the number of molecules per mole equals Avogadro's constant $N_A = 6.02 \times 10^{23}$ mol^{-1}, the specific heat per mole for a monatomic gas is

$$c_V = \frac{3}{2}\kappa_B N_A = \frac{3}{2}R \tag{4.48}$$

where $R(= \kappa_B N_A = 8.314$ J K^{-1} mol^{-1}) is the universal gas constant.

For a diatomic gas, we should consider the contributions from the rotational and vibrational states. We already have from eq. (E.4.1.3) the rotational partition function of one diatomic molecule,

$$Z_r = \sum_{l=0}^{\infty}(2\ell+1)\exp\left[-\frac{\theta_r \ell(\ell+1)}{T}\right] \tag{4.49}$$

We will consider next the vibrational partition function. The vibrational energy of a harmonic oscillator was derived in chapter 2 as

$$E = h\nu\left(n+\frac{1}{2}\right) \quad (n = 0, 1, 2, \ldots) \tag{4.50}$$

The vibrational partition function is thus

$$Z_v = \sum_{n=0}^{\infty}\exp\left(-\frac{h\nu(n+1/2)}{\kappa_B T}\right) = \frac{\exp\left(-\frac{\theta_v}{2T}\right)}{\exp\left(\frac{\theta_v}{T}\right)-1} \tag{4.51}$$

where $\theta_v = h\nu/\kappa_B$ is called the vibrational temperature.

In addition, the molecule also has electronic energy states. From the solution of the electronic energy levels in chapter 2 for a hydrogen atom, we know that the electronic

energy levels are high and that their separations are large. So we can take the first term only of the electronic partition function

$$Z_e = g_{e1}\exp\left[-\frac{E_{e1}}{\kappa_B T}\right] + g_{e2}\exp\left[-\frac{E_{e2}}{\kappa_B T}\right] + \cdots \approx g_{e1}\exp\left[-\frac{E_{e1}}{\kappa_B T}\right] \tag{4.52}$$

where E_{ei} is the ith electronic energy level and g_{ei} is the degeneracy for that energy level. From eqs. (4.27) and (4.32), the canonical partition function for N molecules is

$$Z_N = \frac{(Z_t Z_r Z_v Z_e)^N}{N!} \tag{4.53}$$

and the average internal energy of the molecule, according to eq. (4.30), is thus

$$\begin{aligned} U &= \kappa_B T^2 \frac{\partial}{\partial T}\left\{\ln\left(\frac{(Z_t Z_r Z_v Z_e)^N}{N!}\right)\right\} \\ &= \kappa_B T^2 N\left\{\frac{\partial}{\partial T}(\ln Z_t) + \frac{\partial}{\partial T}(\ln Z_r) + \frac{\partial}{\partial T}(\ln Z_v)\right. \\ &\quad \left. + \frac{\partial}{\partial T}(\ln Z_e) - (\ln N - 1)\right\} \end{aligned} \tag{4.54}$$

The volumetric specific heat can be obtained by taking the derivative of U with respect to T at constant V. The translational energy contribution to the specific heat is given by eq. (4.47). The electronic energy level contribution to the specific heat is

$$C_{V,e} = \frac{N}{V}\frac{\partial}{\partial T}\left[\kappa_B T^2 \frac{\partial}{\partial T}\ln Z_e\right] = 0 \tag{4.55}$$

This result is because the electrons are only sitting in the first energy states and their contribution to the total system energy does not change with temperature. The contribution of rotational energy states to specific heat is

$$C_{V,r} = \frac{N}{V}\frac{\partial}{\partial T}\left[\kappa_B T^2 \frac{\partial}{\partial T}\ln\left(\sum_{\ell=0}^{\infty}(2l+1)\exp\left[-\frac{\theta_r \ell(\ell+1)}{T}\right]\right)\right] \tag{4.56}$$

We know, from eq. (E4.1.3), that the summation in the above equation is proportional to T/θ_r at high temperatures. In this limit, the contribution of the rotational energy level to the specific heat is

$$C_{V,r} = N\kappa_B/V \text{(at high temperature)} \tag{4.57}$$

This result is again a manifestation of the equipartition theorem. A diatomic molecule has two degrees of rotational freedom. So at high temperatures, when the rotational levels are fully excited, each molecule contributes $2 \times \kappa_B T/2 = \kappa_B T$ to the average

energy. At low temperatures, the rotational specific heat must be calculated from the full rotational partition function in the summation format, eq. (4.56). Similarly, the contribution of the vibrational energy state to the specific heat is

$$C_{V,v} = \frac{\kappa_B N}{V}\frac{\theta_v^2}{T^2}\frac{e^{\theta_v/T}}{(e^{\theta_v/T}-1)^2} \tag{4.58}$$

At high temperatures, the above formula leads to

$$C_{V,v} \approx \frac{\kappa_B N}{V} \tag{4.59}$$

which is again a manifestation of the equipartition theorem. After obtaining the contributions from all the energy modes, we calculate the total specific heat of a diatomic molecule by summing each of the contributing terms: $C_V = C_{V,t} + C_{V,r} + C_{V,v} + C_{V,e}$. The following example shows more numerical details.

Example 4.2 *Specific heat of* H_2

The rotational temperature of a hydrogen molecule is 85.3 K and its vibrational temperature is 6332 K. Plot the specific heat of hydrogen gas as a function of temperature.

Solution: From eqs. (4.48), (4.56), and (4.58), we can write the total specific heat per mole of a diatomic gas as

$$\frac{c_V}{R} = \frac{3}{2} + \left(\frac{\theta_v}{T}\right)^2 \frac{e^{\theta_v/T}}{(e^{\theta_v/T}-1)^2} + \frac{\partial}{\partial T}\left[T^2\frac{\partial}{\partial T}\ln\left(\sum_\ell (2\ell+1)\exp\left[-\frac{\theta_r \ell(\ell+1)}{T}\right]\right)\right] \tag{E4.2.1}$$

The last term in the above equation can be written as

$$\frac{c_{V,r}}{R} = \left(\frac{\theta_r}{T}\right)^2 \times \frac{Z_r \sum_\ell (2\ell+1)\ell^2(\ell+1)^2 \exp\left[-\frac{\theta_r\ell(\ell+1)}{T}\right] - \left\{\sum_\ell (2\ell+1)\ell(\ell+1)\exp\left[-\frac{\theta_r\ell(\ell+1)}{T}\right]\right\}^2}{Z_r^2} \tag{E4.2.2}$$

A computer program is used to carry out the above summation. Figure E4.2 plots the variation of c_V/R with temperature. At low temperatures, only the translational energy levels are fully excited and the specific heat is $3R/2$. As the temperature increases, the rotational energy levels become excited and contribute to the specific heat up to a maximum of R so that the total specific heat reaches $5R/2$. At even higher temperatures, the vibrational energy levels start contributing to the specific heat, which approaches a final value of $7R/2$.

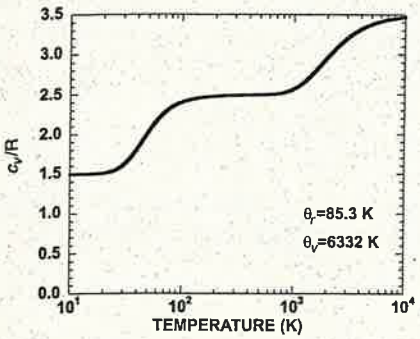

Figure E4.2 Specific heat of H_2 gas as a function of temperature.

4.2.2 Electrons in Crystals

Now we investigate the specific heat of electrons in a crystal. We assume that the electrons have a parabolic band with an isotropic effective mass

$$E - E_c = \frac{\hbar^2}{2m^*}(k_x^2 + k_y^2 + k_z^2) \tag{4.60}$$

We obtained the density of states in chapter 3, eq. (3.52),

$$D(E) = \frac{1}{2\pi^2}\left(\frac{2m^*}{\hbar^2}\right)^{3/2}(E - E_c)^{1/2} \tag{4.61}$$

The total number of electrons per unit volume is thus

$$n = \int_0^\infty f(E,T,\mu)D(E)\,dE \tag{4.62}$$

From eq. (4.62), the chemical potential as a function of temperature can be determined for a given n. For $T = 0$, the above relation leads to

$$n = \int_{E_c}^{\mu} D(E)\,dE = \frac{1}{3\pi^2}\left(\frac{2m^*}{\hbar^2}\right)^{3/2}(\mu - E_c)^{3/2} \tag{4.63}$$

We have already obtained this relation, eq. (3.53), in chapter 3. The chemical potential μ at $T = 0$ is called the Fermi level, E_f.* At other temperatures, eq. (4.62) cannot be explicitly integrated. However, when $(E-\mu)/k_BT \gg 1$, which is the classical limit, we can use the Boltzmann distribution as an approximation of the Fermi–Dirac distribution. Equation (4.62) can be integrated explicitly,

$$n = \int_{E_c}^{\infty} \exp\left(\frac{-E+\mu}{\kappa_B T}\right)\frac{1}{2\pi^2}\left(\frac{2m^*}{\hbar^2}\right)^{3/2}(E - E_c)^{1/2}\,dE = N_c \exp\left(-\frac{E_c - \mu}{\kappa_B T}\right) \tag{4.64}$$

*In electronics, however, E_f is often used to represent the chemical potential at all temperatures.

with

$$N_c = 2\left(\frac{2\pi m^* \kappa_B T}{h^2}\right)^{3/2} \tag{4.65}$$

Equation (4.64) is often used to determine the chemical potential level in doped semiconductors, as will be seen from the following example.

Example 4.3 *Chemical potential level in doped semiconductors*

Silicon is a widely used semiconductor material, and it is often doped with phosphorus to form an n-type semiconductor. Determine the chemical potential of an n-type semiconductor doped with phosphorus with a concentration of 10^{17} cm^{-3} at 300 K, assuming that every phosphorus atom contributes one free electron to the conduction band and neglecting thermally excited electrons from the valence band. Although the silicon conduction bands are not spherical [figure 3.18(b)], they can be approximated by an isotropic band with an effective mass equal to $0.33m$, where m is the free electron mass.

Solution: Silicon has six identical conduction bands [figure 3.18(b)]. When counting all six bands, eq. (4.64) should be written as

$$n = 12\left(\frac{2\pi m * \kappa_B T}{h^2}\right)^{3/2} \exp\left(-\frac{E_c - \mu}{\kappa_B T}\right) \tag{E4.3.1}$$

Taking $n = 10^{17}$ cm^{-3}, we can find the chemical potential as

$$\begin{aligned}\frac{\mu - E_c}{\kappa_B T} &= \ln\left[\frac{n}{12}\left(\frac{2\pi m^* \kappa_B T}{h^2}\right)^{-3/2}\right] \\ &= \ln\left[\frac{10^{23}}{12}\left(\frac{2\pi \times 0.33 \times 9.1 \times 10^{-31} \times 1.38 \times 10^{-23} \times 300}{6.6^2 \times 10^{-68}}\right)^{-3/2}\right] \\ &= -5.65\end{aligned} \tag{E4.3.2}$$

Thus

$$\mu - E_c = -5.65 \times 26 \text{ meV} = -147 \text{ meV} \tag{E4.3.3}$$

Comments. 1. The negative sign means that the chemical potential is below the conduction band edge. The silicon bandgap at room temperature is 1.12 eV. Thus the chemical potential level is within the bandgap. In fact, only in this case, the Boltzmann approximation we used in eq. (4.64) is applicable because the electron energy inside the conduction band, minus the chemical potential, is much larger than $\kappa_B T$. If the chemical potential is close to the band edge or falls inside the conduction band, which is the case when the semiconductors are heavily doped, we need to carry out numerical integration with the Fermi–Dirac statistical distribution.

2. The value of the chemical potential needs a reference point. Equation (4.64) suggests that it is the relative difference between μ and E_c that determines the electron number density, and thus this difference is the value of the chemical potential. In chapter 6 (figure 6.9), we will give a more detailed discussion on the reference point issue.

To calculate the specific heat of electrons, we first formulate the internal energy of electrons as

$$U(T) = \int_{E_c}^{\infty} E f(E, T, \mu) D(E) dE \tag{4.66}$$

For convenience, we limit our discussion to metals so that the number of electrons per unit volume n_e is fixed. We further take $E_c = 0$ as reference, eq. (4.62) becomes

$$n_e = \int_0^{\infty} f(E, T, \mu) D(E) dE = \text{constant} \tag{4.67}$$

We can use eq. (4.67) to rewrite eq. (4.66) as

$$U(T) = \int_0^{\infty} (E - E_f) f(E, T, \mu) D(E) dE + E_f n_e \tag{4.68}$$

where E_f is the Fermi level (μ at $T = 0$ K). In eq. (4.68), since only f is temperature dependent, we obtain the heat capacity of the electron system as

$$C_e = \int_0^{\infty} (E - E_f) \frac{df(E, T, \mu)}{dT} D(E) dE \tag{4.69}$$

Typically, df/dT is nonzero only in the region close to the chemical potential. If the density of states does not vary rapidly around μ, we can use its value at $E = \mu$ and pull $D(\mu)$ out of the integration. In addition, the change of μ with temperature in metal is very small because E_f is very large. We can thus neglect the temperature dependence of μ and set $\mu \approx E_f$. Under these approximations, eq. (4.69) becomes

$$\begin{aligned} C_e &\approx D(\mu) \int_0^{\infty} (E - E_f) \frac{df(E, T, \mu)}{dT} dE \\ &= D(\mu) \int_0^{\infty} \frac{(E - E_f)(E - \mu)}{\kappa_B T^2} \frac{\exp\left(\frac{E-\mu}{\kappa_B T}\right)}{\left[\exp\left(\frac{E-\mu}{\kappa_B T}\right) + 1\right]^2} dE \\ &\approx \kappa_B^2 T D(E_f) \int_{-E_f/\kappa_B T}^{\infty} \frac{x^2 e^x}{(e^x + 1)^2} dx \end{aligned} \tag{4.70}$$

Since $E_f/\kappa_B T$ is very large, the above integral can be evaluated by setting the lower limit to $-\infty$, leading to the following expression for the specific heat

$$C_e = \frac{1}{2}\pi^2 n_e \kappa_B T/T_f \tag{4.71}$$

where $T_f = E_f/\kappa_B$ is called the *Fermi temperature*. In deriving eq. (4.71), we used the relationship $n_e = 2E_f D(E_f)/3$, which can be obtained from eqs. (3.52) and (3.53). Thus the specific heat of electrons is linearly dependent on temperature.

4.2.3 Phonons

4.2.3.1 Debye Model

In chapter 3, we obtained the phonon density of states per unit volume under the Debye approximation when the three acoustic phonon polarizations are identical [eq. (3.55)],

$$D(\omega) = \frac{dN}{V\,d\omega} = 3 \times \frac{\omega^2}{2\pi^2 v_D^3} \tag{4.72}$$

The total energy of phonons per unit volume is

$$U = \int_0^{\omega_D} \hbar\omega f\,(T,\omega) D\,(\omega)\,d\omega = \frac{3}{2\pi^2 v_D^3} \int_0^{\omega_D} \frac{\hbar\omega^3 d\omega}{\exp(\hbar\omega/\kappa_B T) - 1} \tag{4.73}$$

and the volumetric specific heat of phonons can be calculated from

$$C = \frac{\partial U}{\partial T} = \frac{3\hbar^2}{2\pi^2 v_D^3 \kappa_B T^2} \int_0^{\omega_D} \frac{\omega^4 \exp\,(\hbar\omega/\kappa_B T)}{[\exp(\hbar\omega/\kappa_B T) - 1]^2}\,d\omega \tag{4.74}$$

From eqs. (3.56) and (3.57), the Debye frequency ω_D, Debye velocity v_D, and Debye temperature θ_D are related through

$$\omega_D = \frac{\pi v_D}{a_D} = \frac{\kappa_B \theta_D}{\hbar} \tag{4.75}$$

where a_D is the effective lattice constant under the Debye model. Substituting eq. (4.75) into eq. (4.74), we get

$$C = \frac{3\hbar^2}{2\pi^2 (a_D \omega_D/\pi)^3 \kappa_B T^2} \int_0^{\omega_D} \frac{\omega^4 \exp(\hbar\omega/\kappa_B T)}{[\exp\,(\hbar\omega/\kappa_B T) - 1]^2}\,d\omega$$

$$= \frac{3\pi\kappa_B}{2a_D^3} \left(\frac{T}{\theta_D}\right)^3 \int_0^{\theta_D/T} \frac{x^4 e^x dx}{(e^x - 1)^2} \tag{4.76}$$

Using eq. (3.57), the specific heat can be further written as

$$C = 9\kappa_B \left(\frac{N}{V}\right) \left(\frac{T}{\theta_D}\right)^3 \int_0^{\theta_D/T} \frac{x^4 e^x dx}{(e^x - 1)^2} \tag{4.77}$$

where N/V is the number of atoms per unit volume. At low temperatures, the integration limit can be set to infinity, leading to the familiar T^3 law,

$$C(T) = \frac{36\pi^4 \kappa_B}{15} \left(\frac{N}{V}\right) \left(\frac{T}{\theta_D}\right)^3 \propto T^3 \tag{4.78}$$

Generally, the Debye temperature is unknown and the above expression is used to calculate the Debye temperature from experimentally measured values of specific heat. If the Debye model is accurate, a single value of the Debye temperature should be able to fit all of the temperature-dependent specific heat data. Such a situation happens rarely, however, and the Debye temperature is sometimes given as a function of temperature. This temperature-dependent Debye temperature is because the Debye model assumes a linear dispersion, which is not valid for phonons close to the boundary of the first Brillouin zone. In particular, it is completely wrong for optical phonons, for which the Einstein model is more appropriate, as we discuss below.

4.2.3.2 Einstein Model

Einstein's model assumes that all phonons have the same frequency ω_E and is thus more appropriate for optical phonons. We assume that there are N' states; that is, N' is the number of lattice points or primitive cells for each optical phonon polarization.* The total energy of the crystal per unit volume due to the contribution of the optical phonons with a frequency ω_E is then

$$U = N_p \frac{N' f(T,\omega_E)\hbar\omega_E}{V} = \frac{N_p N' \hbar\omega_E}{V[\exp(\hbar\omega_E/\kappa_B T) - 1]} \tag{4.79}$$

where the factor N_p accounts for the number of polarizations of optical phonons at this frequency. The specific heat per unit volume is then

$$C = \frac{\partial U}{\partial T} = N_p \kappa_B \frac{N'}{V} \frac{(\hbar\omega_E/\kappa_B T)^2 \exp\,(\hbar\omega_E/\kappa_B T)}{[\exp(\hbar\omega_E/\kappa_B T_B) - 1]^2} \tag{4.80}$$

The contributions of other optical phonons at a different frequency can be similarly calculated. At high temperature, both the Debye model and the Einstein model lead to the same result, as required by the equipartition theorem because the oscillator has three directions and each direction has two degrees of freedom (kinetic energy plus potential energy).

Clearly, the Debye model will be more appropriate for acoustic phonons and the Einstein model for optical phonons. At low temperatures, acoustic phonons are normally

*Notice that this N' is different from N in the Debye model, in which all phonon modes (including the optical modes) are lumped as three identical acoustic modes.

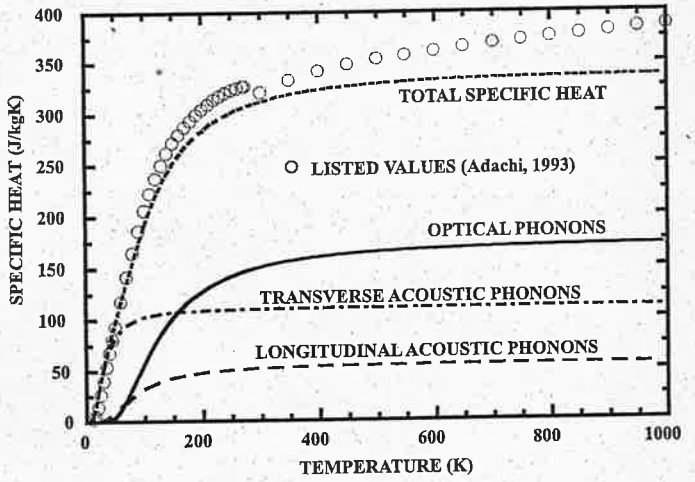

Figure 4.5 Estimated contribution of different phonon branches to the specific heat of GaAs (Chen, 1997).

excited, so the Debye approximation is more appropriate. At room and higher temperatures, both acoustic and optical phonons are excited and a combination of the two models is more appropriate. Figure 4.5 shows the estimated contributions of different phonon polarizations to the specific heat of GaAs (Chen, 1997). In this figure, a sine-function was assumed for the acoustic phonon dispersion.

4.2.4 Photons

Photons are bosons and obey the Bose–Einstein distribution. We have obtained the photon density of states in a three-dimensional cavity in eq. (3.59),

$$D(\omega) = \frac{dN}{V\,d\omega} = \frac{\omega^2}{\pi^2 c^3} \tag{4.81}$$

From eq. (4.81), the photon energy density per unit volume per unit angular frequency interval is

$$U_\omega = f(\omega, T)\hbar\omega D(\omega) = \frac{\hbar}{\pi^2 c^3}\frac{\omega^3}{[\exp(\hbar\omega/\kappa_B T) - 1]} \tag{4.82}$$

Since a photon propagates in all directions at the speed of light c, the intensity is then*

$$I_\omega = \frac{cU_\omega}{4\pi} = \frac{\hbar}{4\pi^3 c^2}\frac{\omega^3}{[\exp(\hbar\omega/\kappa_B T) - 1]} \tag{4.83}$$

*See section 6.1.3 for a more detailed explanation of intensity.

Equation (4.83) is the Planck blackbody radiation law, expressed in terms of per angular frequency interval. In terms of wavelength, we have

$$I_\lambda = I_\omega\left|\frac{d\omega}{d\lambda}\right| = \frac{C_1/\pi}{\lambda^5[\exp(C_2/\lambda T) - 1]} \tag{4.84}$$

where $C_1 = 2\pi hc^2$ and $C_2 = hc/\kappa_B$. The blackbody emissivity power that is given in eq. (1.9) can be obtained easily from the above expression for intensity through $e_\lambda = \pi I_\lambda$. Integration of eq. (4.82) for frequencies ranging from 0 to ∞ leads to the total photon energy density

$$U = \frac{4}{c}\sigma T^4 \tag{4.85}$$

where $\sigma (= 5.67 \times 10^{-8}\ \mathrm{W\,m^{-2}\,K^{-4}})$ is the Stefan–Boltzmann constant. The total intensity is

$$I = \frac{\sigma T^4}{\pi} \tag{4.86}$$

and the blackbody emissive power is thus

$$e_b = \pi I = \sigma T^4 \tag{4.87}$$

Although the concept of specific heat is seldom used in radiation, we can follow the previous treatment for electrons and phonons and calculate the photon specific heat,

$$C = \frac{16\sigma T^3}{c} \tag{4.88}$$

which has the same temperature dependence as the specific heat of phonons at low temperatures [eq. (4.78)].

Example 4.4 *Electron and phonon contributions to specific heat*

The Debye temperature of gold is 170 K and its Fermi level is 5.53 eV. Compute the specific heat of phonons and electrons in the temperature range of 0–1000 K.

Solution: The phonon and electron contributions to specific heat are given by

$$\text{Phonon: } C = 9\kappa_B\left(\frac{N}{V}\right)\left(\frac{T}{\theta_D}\right)^3\int_0^{\theta_D/T}\frac{x^4 e^x\,dx}{(e^x - 1)^2}$$

$$\text{Electron: } C_e = \frac{1}{2}\pi^2 n_e \kappa_B T/T_f$$

Gold has an fcc structure with a lattice constant of 4.08 Å, and the number of atoms per unit cell is 4. Each atom contributes one valence electron. We have $n_e = N/V = 4/(4.08)^3 \times 10^{-30}\ \mathrm{m^{-3}}$. The Fermi temperature $T_f = E_f/k_B = 64{,}115$ K. Substituting these numbers into the above expressions, we obtain the phonon

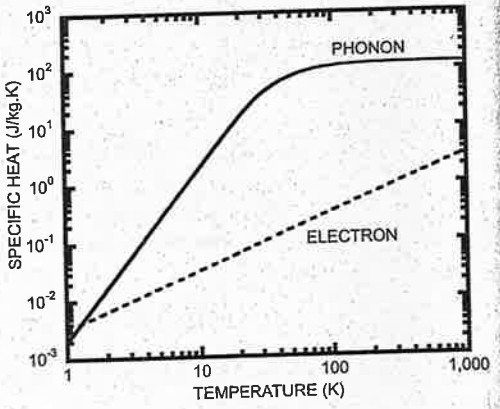

Figure E4.4 Phonon and electron contributions to the specific heat of gold.

and electron specific heats. The volumetric specific heats are converted into mass specific heat ($c = C/\rho$) and plotted in figure E4.4. We observe that the electron specific heat is typically much smaller than the phonon specific heat, except at very low temperatures.

4.3 Size Effects on Internal Energy and Specific Heat

In nanostructures, we expect that the internal energy and specific heat will be different from what we have given in the preceding sections. The differences come from two sources: one is physical and the other is mathematical. On the physics side, the energy levels, and their associated densities of states, will differ from those in bulk materials, as we have seen in chapter 3. On the mathematical side, for bulk materials we have replaced the summation over all energy states by integration in calculating the total energy. For nanostructures, this approximation may no longer be accurate.

A few experimental and theoretical studies exist about the size effects on the phonon specific heat of nanostructures. For systems of dimensionality d of 1 or higher ($d = 1$ for nanowires, $d = 2$ for films, and $d = 3$ for bulk structures), the Debye model predicts that at low temperatures the lattice specific heat should be proportional to T^d. The most common criterion for dimensional crossover is to compare the average phonon wavelength λ to the length scale of the structure. The average phonon wavelength can be estimated from the spectral-dependent phonon internal energy [the integrand of eq. (4.73)], similar to that obtaining the Wien's displacement law, eq. (1.11), from the Planck law. Well below the Debye temperature, this wavelength is given by $\lambda T \approx 50$ nm K for sound velocity v_s (5000 m s^{-1}). For example, a 3 nm Si thin film would be expected to exhibit $C \sim T^3$ behavior at 50 K ($\lambda \approx 1$ nm), but $C \sim T^2$ behavior at 5 K ($\lambda \approx 10$ nm). Some questions exist about whether the resulting low-dimensional specific heat should be larger or smaller than the corresponding bulk value. A simple model (Dames et al., 2004) summing over all of the normal modes of an elastic continuum with free boundaries predicts that the low-temperature specific heat of

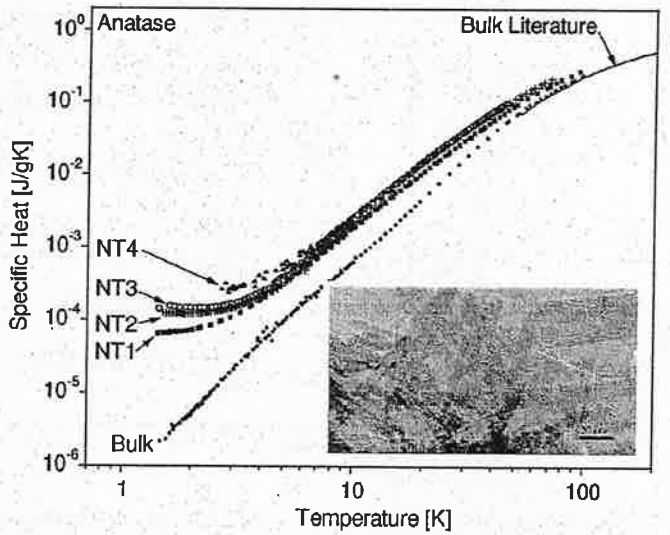

Figure 4.6 Experimental specific heat of anatase TiO_2 nanotubes (four kinds of tubes synthesized under different conditions) and that of bulk TiO_2 (Dames et al., 2004). Insert shows transmission electron micrographs of the nanotubes.

1- or 2-dimensional systems should exceed the bulk value, but several other calculations predict the low-temperature, low-dimensional specific heat should be reduced compared to bulk (Prasher and Phelan, 1998; Yang and Chen, 2000), slightly larger than the bulk value (Grille et al., 1996), or varying from both below and above bulk (Hotz and Siems, 1987; Tosic et al., 1992).

Limited experimental data are available to test these theories. The first studies were on zero-dimensional (0D) metallic nanoparticles of ~2–10 nm diameter, where experiments (Novotny and Meincke, 1973; Chen et al., 1995) show a specific heat enhanced by 50–100% at temperatures where the average phonon wavelength is comparable to the diameter of the nanoparticles, an exponential decay at lower temperatures, and an asymptotic return to bulk values at higher temperatures. These results have been successfully explained by theories that sum over all of the normal modes of an elastic sphere with free boundaries (Baltes and Hilf, 1973; Lautenschlager, 1975; Nonnenmacher, 1975). For anatase nanoparticles, Wu et al. (2001) reported enhancement by 20% for particles of about 15 nm diameter between 78 K and 370 K. In figure 4.6, we compare the experimental data on the specific heat of compacted titanium dioxide (TiO_2) nanotubes with that of bulk TiO_2, and show that the nanotubes have higher specific heat at low temperatures (Dames et al., 2004).

Considerable effort has been devoted to studying the specific heat of carbon nanotubes (CNT). Yi et al. (1999) observed a linear temperature dependence down to 10 K in multi-walled (MW) CNT, in close agreement with isolated sheets of graphene. In contrast, another MWCNT experiment by Mizel et al. (1999) showed a much steeper decay, with temperatures of about $T^{2.5}$ down to ~1 K, a better match to graphite. Bundles of

single-walled (SW) CNT were studied by both Hone et al. (2000) and Mizel et al. (1999), and exhibited a linear or slightly superlinear temperature dependence from ~100 K down to ~2–4 K. At lower temperatures, Lasjaunias et al. (2003) reported a transition to T^3 attributed to the filling up of inter-tube modes, plus a surprising additional term proportional to $T^{0.34}$ or $T^{0.62}$ below ~1 K that was qualitatively attributed to localized excitations of atomic rearrangement as in glasses and amorphous materials. In all of these CNT, the specific heat is bounded between that of graphite and graphene. Various theoretical efforts have had mixed success at explaining these MWCNT and SWCNT measurements by extending isolated tube models to include the effects of interlayer coupling (in MWCNT) and intertube coupling (Mizel et al., 1999; Hone et al., 2000; Zhang et al., 2003). Overall, more work is needed to reconcile the diverse experimental results with theory (Dresselhaus and Eklund, 2000).

In comparison with phonons, we anticipate that the specific heat of electrons will have a stronger size dependence, due to the following factors: (1) the energy quantization of electrons is more dramatic than that of phonons; (2) the specific heat also depends on the Fermi level, particularly the rate of change of the density of states at the Fermi level. In our derivation of the electron specific heat in metals, we assumed that the density of states does not change much near the Fermi level. For nanostructures, the sharp features in the electronic density of states suggest that this assumption may not be valid. Indeed, existing studies show that the specific heat is a strong function of the size (Ghatak and Biswas, 1994; Lin and Shung, 1996).

For photons, we are not interested in the specific heat but rather in the energy density or emission spectrum from small objects. Since thermal radiation can have relatively long wavelengths, the issue of size effects on the energy density of the emission spectrum from a small object has been studied for various geometries (Rytov, 1959; Rytov et al., 1989). One interesting question is whether the thermal emission from any structure at any specific wavelength can exceed the blackbody radiation given by the Planck law. For example, the density of states in photonic crystals can be very different from that in free space. It can be inferred that in the frequency region where the photon density of states of the photonic crystal is larger than that in its parent crystal, the energy density of the thermal radiation inside the photonic crystal can exceed that in its parent crystal. However, not all of the energy can be emitted into free space since the density of states in free space is limited by eq. (4.81), and thus the maximum emissive power in an open free space is the blackbody radiation. There are, however, some recent experimental reports of the far-field thermal emission from photonic crystals being larger than that of the blackbody, although the physics is not clear (Lin et al., 2003). At small scales, however, radiative heat exchange can exceed that between two blackbodies due to the tunneling of evanescent and surface waves (Polder and Van Hove, 1971; Tien and Cunnington, 1973; Pendry, 1999; Mulet et al.; 2002; Narayanaswamy and Chen, 2003), which we will discuss in more detail in the next chapter. Another example is that the emissivity of particles with a diameter comparable to the wavelength can exceed 1 because of the diffraction effect (Bohren and Huffman, 1983).

4.4 Summary of Chapter 4

Through statistical mechanics, this chapter establishes the link between the energy states and temperature for a system in equilibrium. A system in equilibrium makes

rapid transitions among accessible quantum states as a function of time. A fundamental assumption in statistical mechanics is that, in an isolated system, every accessible quantum state has an equal probability of being sampled by the system. Because it is hard to follow the time evolution of the system, we use an ensemble average to replace the time average for quantities of interest and assume that the ensemble average equals the time average. This assumption is called the egordicity assumption. An ensemble is made from a collection of systems, each of which is one accessible quantum state of the original system (but is stationary). Depending on the macroscopic constraints for the original system, we can establish different ensembles. We discussed the following three ensembles.

A *microcanonical ensemble* corresponds to an original system that is isolated with fixed U, V, and N. Each system in the ensemble represents one accessible quantum state in the original system. The most important relation for such an ensemble is the Boltzmann principle, which relates the total number of quantum states Ω of the original system (and thus the number of systems in the ensemble) to the entropy of the system,

$$S(U, V, N) = \kappa_B \ln \Omega \tag{4.89}$$

Through the Boltzmann principle and the first law of thermodynamics, we can obtain other thermodynamic properties of the system,

$$\frac{1}{T} = \left(\frac{\partial S}{\partial U}\right)_{V,N}, \frac{p}{T} = \left(\frac{\partial S}{\partial V}\right)_{U,N}, -\frac{\mu}{T} = \left(\frac{\partial S}{\partial N}\right)_{U,V} \tag{4.90}$$

Thus S is the thermodynamic potential of a microcanonical ensemble and its natural variables are U, V, and N.

A *canonical ensemble* is more appropriate for a system with fixed T, V, and N. In this case, the system can exchange energy with its surroundings and we assumed that the surroundings are a thermal reservoir. Although we can combine the system and the reservoir to establish a microcanonical ensemble for the combined system, it is more convenient to establish a canonical ensemble in which each of the systems is an accessible quantum state of the original system and each can exchange energy with the reservoir. Since a number of accessible quantum states exists in the reservoir corresponding to one specific accessible quantum state of the system, the probability of observing any one system in the canonical ensemble is no longer equal, as in a microcanonical system. The probability of finding a quantum state with energy E_i is

$$P(E_i) = e^{-E_i/\kappa_B T}/Z \text{ where } Z = \sum_i \exp\left[-\frac{E_i}{\kappa_B T}\right] \tag{4.91}$$

In eq. (4.91), $e^{-E_i/\kappa_B T}$ is the familiar Boltzmann factor and Z is called the canonical partition function. The canonical partition function is related to the Helmholtz free energy, a thermodynamic potential with natural variables as T, V, and N, through

$$F(T, V, N) = U - TS = -\kappa_B T \ln Z \tag{4.92}$$

If, rather than having N fixed, we consider a system with fixed T, V, and μ, such a system exchanges not only energy but also particles with its reservoir. We can construct an the ensemble that consists of a number of systems, each corresponds to one accessible

quantum states in the original system and can exchange energy and particles with the reservoir. This ensemble is called the *grand canonical ensemble*, and the probability of finding a particular system with energy E_i and number of particles N_i is given by

$$P(E_i, N_i) = \frac{\exp\left[\frac{N_i\mu - E_i}{\kappa_B T}\right]}{\Im} \tag{4.93}$$

where the exponential is called the Gibbs factor and

$$\Im(T, V, \mu) = \sum_{N_i}\sum_{E_i} \exp\left[\frac{N_i\mu - E_i}{\kappa_B T}\right] = \sum_{N_i} \lambda^{N_i} Z_i \tag{4.94}$$

is the grand canonical partition function.

After establishing the probabilities and partition functions for different ensembles, we applied them to different particles. The partition function for a dilute gas made of N indistinguishable molecules is given by

$$Z_N = \frac{(Z_t Z_r Z_v Z_e)^N}{N!} \tag{4.95}$$

where Z_t, Z_r, Z_v, and Z_e are the partition functions for the translational, the rotational, the vibrational, and the electronic states, respectively.

For electrons and other fermions, the average number of particles in a specific accessible quantum state with an energy E is given by the Fermi–Dirac distribution function,

$$f(E, T, \mu) = \frac{1}{\exp\left(\frac{E-\mu}{\kappa_B T}\right) + 1} \tag{4.96}$$

On the basis of f, we can calculate the amount of energy this quantum state contributes to the total energy as $\langle E\rangle = E \times f$.

For phonons, photons, and other bosons, the average number of particles in a specific quantum state with frequency ν is given by the Bose–Einstein distribution

$$f(\nu, T) = \frac{1}{\exp\left(\frac{h\nu}{\kappa_B T}\right) - 1} \tag{4.97}$$

Given this average number of particles, each having an energy $h\nu$, we can calculate the contribution of this specific accessible quantum state to the total system energy as $\langle E\rangle = h\nu f$.

In the classical limit, when the exponential in these distributions is much larger than one, both Bose–Einstein and Fermi–Dirac distributions reduces to the classical Boltzmann distribution

$$f(E, T, \mu) = \exp\left(-\frac{E-\mu}{\kappa_B T}\right) \tag{4.98}$$

With the distribution functions, we are in a position to count the energy of the system, from which other properties related to the energy, such as the specific heat for electrons and phonons and the emissive power for blackbody radiation, can be determined. Since, at each allowable energy level, the system can be degenerate as measured by the density of states $D(E)$, the total energy at this level is $U(E) = E \times f \times D(E)$. If we want the total energy of the system, we should sum $U(E)$ over all energy levels. In a three-dimensional space (bulk materials), the summation is often replaced by integration since the separation between energy levels is usually very small. This procedure leads to the following results for electrons, phonons, and photons:

Electron specific heat: $C_V \propto T$ (4.99)

Phonon specific heat: $C_V \propto T^3$ (at low temperature) (4.100)

$C_V =$ constant (at high temperatures) (4.101)

Photon emissive power: $I_\omega = \frac{\hbar}{4\pi^3 c^2} \frac{\omega^3}{[\exp(\hbar\omega/\kappa_B T) - 1]}$ (Planck's law) (4.102)

For nanostructures, the statistical distributions are still valid as long as the systems are in thermal equilibrium. However, there are several reasons that could invalidate the derivations of the specific heat and emissive power for bulk materials. One is that the energy levels are different in nanostructures from these in macrostructures, which will change the density of states. Second is that the energy separation is usually large and the replacement of the summation by integration over energy is no longer valid as it was for bulk materials.

With the contents of this chapter and the previous two chapters, the readers are encouraged to read through current literature. With persistency and patience, readers may find that they begin to understand (or partially understand) some of the nanoscience and nanotechnology research topics.

4.5 Nomenclature for Chapter 4

a	lattice constant, m
c	speed of light
c_v	specific heat per mole, J K^{-1} mol^{-1}
C	volumetric specific heat, J m^{-3} K^{-1}
D	density of states per unit volume, m^{-3}
e_b	blackbody radiation emissive power, W m^{-2}
E	energy, J
E_c	conduction band edge, J
E_f	Fermi level, J
f	distribution function
F	Helmholz free energy, J
G	grand canonical potential, J
h	Planck constant, J s
$\hbar$	Planck constant divided by 2π, J s
I	intensity, W m^{-2} srad^{-1}
k	magnitude of wave vector, m^{-1}
L	length of box, m
m	mass, kg
m^*	effective mass, kg
n	quantum number; electron number density, m^{-3}
N	total number of particles in the system
N_A	Avogadro constant, mol^{-1}
N_p	number of polarization of optical phonons

R	universal gas constant, $J\,K^{-1}\,mol^{-1}$	ω	angular frequency, rad.Hz
s	accessible quantum state	Ω	number of accessible states in a microcanonical system
S	entropy, $J\,K^{-1}$		
T	temperature, K	$\mathfrak{Z}$	grand canonical partition function
U	system energy, J		
v	speed, $m\,s^{-1}$	$\langle\rangle$	ensemble average
V	system volume, m^3		
x	integration variable	Subscripts	
Z	canonical partition function		
θ	temperature, K	D	Debye
κ_B	Boltzmann constant, $J\,K^{-1}$	e	electronic
λ	thermal de Broglie wavelength, m	f	at Fermi level
		i	ith energy level
μ	chemical potential, J	r	reservoir; rotational
ν	frequency of phonons or photons, Hz	t	total
		v	vibrational
ρ	density, $kg\,m^{-3}$	V	constant volume
σ	Stefan–Boltzmann constant, $W\,m^{-2}\,K^{-4}$	x, y, z	Cartesian coordinate direction

4.6 References

Adachi, S., ed., 1993, *Properties of Aluminum Gallium Arsenide*, INSPEC, London.

Baltes, H.P., and Hilf, E.R., 1973, "Specific Heat of Lead Grains," *Solid State Communications*, vol. 12, pp. 369–373.

Bohren, C.F., and Huffman, D.R., 1983, Absorption and Scattering of Light by Small Particles, Wiley, New York.

Callen, H.B., 1985, *Thermodynamics and an Introduction to Thermostatistics*, Wiley, New York.

Chen, Y.Y., Yao, Y.D., Hsiao, S.S., Jen, S.U., Lin, B.T., Lin, H.M., and Tung, C.Y., 1995, "Specific Heat Study of Nanocrystalline Palladium," *Physical Review B*, vol. 52, pp. 9364–9369.

Chen, G., 1997, "Size and Interface Effects on Thermal Conductivity of Superlattices and Periodic Thin-Film Structures," *Journal of Heat Transfer*, vol. 119, pp. 220–229.

Dames, C., Poudel, B., Wang, W.Z., Huang, J.Y., Ren, Z.F., Sun, Y., Oh, J.I., Opeil, C., Naughton, S.J., Naughton, M.J., and Chen, G., "Low-dimensional phonon specific heat of titanium dioxide nanotubes," submitted for publication.

Dresselhaus, M.S., and Eklund, P.C., 2000, "Phonons in Carbon Nanotubes," *Advances in Physics*, vol. 49, pp. 705–814.

Ghatak, K., and Biswas, S., 1994, "Influence of Quantum Confinement on the Heat Capacity of Graphite," *Fizika A*, vol. 3, pp. 7–24.

Grille, H., Karch, K., and Bechstedt, F., 1996, "Thermal Properties of $(GaAs)_N(Ga_{1-x}Al_xAs)_N(001)$ Superlattices," *Physica B*, vol. 119–120, pp. 690–692.

Hone, J., Batlogg, B., Benes, Z., Johnson, A.T., and Fischer, J.E., 2000, "Quantized Phonon Spectrum of Single-Wall Carbon Nanotubes," *Science*, vol. 289, pp. 1730–1733.

Hotz, R., and Siems, R., 1987, "Density of States and Specific Heat of Elastic Vibrations in Layer Structures," *Superlattices and Microstructures*, vol. 3, pp. 445–454.

Kittel, C., and Kroemer, H., 1980, *Thermal Physics*, 2nd ed., Freeman, New York.

Kubo, R., Toda, M., and Hashitsume, N., 1998, *Statistical Physics II*, 2nd ed., Springer, Berlin.

Lasjaunias, J.C., Biljakovic, K., Monceau, P., and Sauvajol, J.L., 2003, "Low-Energy Vibrational Excitations in Carbon Nanotubes Studied by Heat Capacity," *Nanotechnology*, vol. 14, pp. 998–1003.

Lautenschlager, R., 1975, "Improved Theory of the Vibrational Specific Heat of Lead Grains," *Solid State Communications*, vol. 16, pp. 1331–1334.

Lin, M.F., and Shung, W.W.K., 1996, "Electronic Specific Heat of Single-Walled Carbon Nanotubes," *Physical Review B*, vol. 54, pp. 2896–2900.

Lin, S.Y., Moreno, J., and Fleming, J.G., 2003, "Three-Dimensional Photonic-Crystal Emitters for Thermal Photovoltaic Power Generation," *Applied Physics Letters*, vol. 83, pp. 380–381.

Mizel, A., Benedict, L.X., Cohen, M.L., Louie, S.G., et al., 1999, "Analysis of the Low-Temperature Specific Heat of Multiwalled Carbon Nanotubes and Carbon Nanotube Ropes," *Physical Review B*, vol. 60, pp. 3264–3270.

Mulet, J.-P., Joulain, K.L., Carminati, R., and Greffet, J.-J., 2002, "Enhanced Radiative Heat Transfer at Nanometric Distances," *Microscale Thermophysical Engineering*, vol. 6, pp. 209–222.

Narayanaswamy, A., and Chen, G., 2003, "Surface Modes for Near-Field Thermophotovoltaics," *Applied Physics Letters*, vol. 82, pp. 3544–3546.

Nonnenmacher, Th.F., 1975 "Quantum Size Effect on the Specific Heat of Small Particles," *Physics Letters A*, vol. 51, pp. 213–214.

Novotny, V., and Meincke, P.P.M., 1973, "Thermodynamic Lattice and Electronic Properties of Small Particles," *Physical Review B*, vol. 8, pp. 4186–4199.

Pendry, J.B., 1999, "Radiative Exchange of Heat between Nanostructures," *Journal of Physics, Condensed Matter*, vol. 11, pp. 6621–6633.

Polder, D., and Van Hove, M., 1971, "Theory of Radiative Heat Transfer between Closely Spaced Bodies," *Physical Review B*, vol. 4, pp. 3303–3314.

Prasher, R.S., and Phelan, P.E., 1998, "Size Effects on the Thermodynamic Properties of Thin Solid Films," *Journal of Heat Transfer*, vol. 120, pp. 1078–1086.

Rytov, S.M., 1959, *Theory of Electric Fluctuations and Thermal Radiation*, Air Force Cambridge Research Center, Bedford, MA, Report AFCRC-TR-59–162.

Rytov, S.M., Kravtsov, Y.A., and Tatarskii, V.I., 1989, *Principles of Statistical Radiophysics*, vol. 3, Springer-Verlag, Berlin.

Tien, C.L., and Cunnington, G.R., 1973, "Cryogenic Insulation Heat Transfer," *Advances in Heat Transfer*, vol. 9, pp. 349–417.

Tosic, B.S., Setrajcic, J.P., Mirjanic, D.L., and Bundalo, Z.V., 1992, "Low-Temperature Properties of Thin Films," *Physica A*, vol. 184, pp. 354–366.

Wu, X.M., Wang, L., Tan, Z.C., Li, G.H., and Qu, S.S., 2001, "Preparation, Characterization, and Low-Temperature Heat Capacities of Nanocrystalline TiO_2 Ultrafine Powder," *Journal of Solid State Chemistry*, vol. 156, pp. 220–223.

Yang, B., and Chen, G., 2000, "Lattice Dynamics Study of Phonon Heat Conduction in Quantum Wells," *Physics of Low-Dimensional Structures*, vol. 5/6, pp. 37–48.

Yi, W., Lu, L., Zhang, D.-L., Pan, Z.W., and Xie, S.S., 1999, "Linear Specific Heat of Carbon Nanotubes," *Physical Review B*, vol. 59, pp. R9015–R9018.

Zhang, S., Xia, M., Zhao, S., Xu, T., and Zhang, E., 2003, "Specific Heat of Single-Walled Carbon Nanotubes," *Physical Review B*, vol. 68, 075415/1–7.

4.7 Exercises

4.1 *Grand canonical ensemble.* Establish a grand canonical ensemble and derive the probability distribution for the ensemble, that is, eq. (4.17).

4.2 *Thermal de Broglie wavelength.* Calculate the thermal de Broglie wavelength of a He molecule at 300 K and show that the dilute gas condition, eq. (4.34), is satisfied at 1 atm and 300 K.

4.3 *Specific heat of monatomic gas.* Derive an expression for the specific heat of a box of He gas and plot it as a function of temperature.

4.4 *Entropy of mixing.* There are two tanks of gas. Both tanks have N molecules and a volume V, and are at the same temperature and pressure. The two tanks are connected by a pipe with a valve. After the valve is opened, the gases in both tanks eventually mix into a homogeneous mixture. Show the following:

(a) If the two gases are identical, there is no change in entropy due to the mixing.

(b) If the two gases are different, the mixing causes an entropy production of $2N \ln 2$.

The difference in the results is called the Gibbs paradox and comes from the distinguishability of the molecules.

4.5 *Bose–Einstein distribution.* Plot the Bose–Einstein distribution as a function of frequency for $T = 100$ K, 300 K, and 1000 K. Compare with the Boltzmann distribution at the same temperatures.

4.6 *Electrons in semiconductors.* A semiconductor has a parabolic band structure

$$E - E_c = \frac{\hbar^2}{2m^*}(k_x^2 + k_y^2 + k_z^2)$$

The Fermi level in the semiconductor could be above or below the conduction band edge. Take the electron effective mass as the free electron mass. For $\mu - E_c = 0.05$ eV and $T = 300$ K, do the following in the range $0.0\,\text{eV} < E - E_c < 0.1\,\text{eV}$:

(a) Plot the Fermi–Dirac distribution as a function of E,

(b) Plot the density of states as a function of E,

(c) Calculate the product of $f(E,T)D(E)$, which means the average number of electrons at each E, and plot the product as a function of E,

(d) Calculate the product of E_f(E,T)D(E), which means the actual energy at each allowable energy level, and plot the product as a function of E.

Repeat the questions for $\mu - E_c = -0.05$ eV.

4.7 *Chemical potential.* The number of electrons in the conduction band can be assumed to be equal to the dopant concentration. Calculate the chemical potential levels relative to the band edge for the dopant concentrations of 10^{18} cm^{-3} and 10^{19} cm^{-3}, assuming free electron mass and $T = 300$ K.

4.8 *Debye crystal.* A crystal has a Debye velocity of 5000 m s^{-1}, and a Debye temperature of 500 K. For $T = 300$ K,

(a) Plot the Bose–Einstein distribution as a function of ω,

(b) Plot the density of states as a function ω using the Debye model.

(c) Plot fD as a function of frequency ω.

(d) Plot $\hbar\omega fD$ as a function of ω.

(e) Compute the specific heat of the crystal as a function of temperature for $1 < T < 1000$ K.

4.9 *Blackbody radiation.* Consider the blackbody radiation at $T = 300$ K.

(a) Plot the Bose–Einstein distribution as a function of angular frequency ω.

(b) Plot the density of states as a function of ω, using the Debye model.

(c) Plot fD as a function of ω.

(d) Plot $\hbar\omega fD$ as a function of ω.

(e) Compute the emissive power as a function of temperature and the corresponding specific heat.

(f) Also compare (a)–(e) with corresponding questions for phonons in problem 4.8.

4.10 *Specific heat of diatomic molecules.* A diatomic molecule has one rotational energy state at 100 meV and one vibrational energy state at 1 eV. Plot the contribution of this molecule to the specific heat of a box of such molecules as a function of temperature.

4.11 *Electron specific heat of a quantum well.* Derive and plot the electron internal energy and specific heat for an infinite-barrier-height quantum well, $L_z = 20$ Å and 100 Å, as a function of temperature. Take the electron effective mass equal to the free electron mass and an electron density $n_e = 2 \times 10^{28}$ m^{-3}.

4.12 *Electron specific heat of quantum dots.* Derive and plot the electron internal energy and specific heat for a cubic quantum dot with infinite potential barrier height with $L = 20$ Å or 100 Å as a function of temperature. Take the electron effective mass equal to the free electron mass and an electron density $n_e = 2 \times 10^{28}$ m^{-3}.

4.13 *Phonon specific heat.* Assuming that phonons obey the following dispersion relation (three-dimensional isotropic medium)

$$\omega = 2\sqrt{\frac{K}{m}}\left|\sin\frac{|\mathbf{k}|a}{2}\right|$$

where a is the lattice constant, K the spring constant, and $\mathbf{k}$ the wavevector. Derive an expression for the phonon internal energy and specific heat.

4.14 *Fermi level and specific heat in Au.* The valence electron concentration in gold is 5.9×10^{22} cm^{-3}.

(a) Calculate the Fermi level in gold at zero temperature.

(b) What is the corresponding Fermi temperature?

(c) Estimate the electronic contribution to the specific heat of gold at 300 K.

(d) Calculate the Fermi level at 300 K.

4.15 *Phonon specific heat in Ge.* Germanium has an fcc structure with two Ge atoms per basis and a lattice constant of 5.66 Å. On the basis of the equipartition theorem, estimate the phonon specific heat per unit mass in germanium at high temperatures and compare it with the experimental specific heat value at 300 K.

4.16 *Phonon high temperature specific heat—Debye model.* Prove that at high temperatures the Debye model leads to a specific heat of $3k_BN$, where N is the number of atoms in the crystal.

4.17 *Diamond specific heat.* The Debye temperature of diamond is 1320 K. Calculate the specific heat of diamond at 300 K and compare it with the literature value (the lattice constant of diamond is 3.567 Å).

4.18 *Phonon specific heat in a quantum dot.* A bulk crystal has a Debye velocity of 5000 m s^{-1} and a Debye temperature of 300 K. Assuming that phonons in a quantum dot obey the same dispersion relation as those in the bulk material, but considering the discrete nature of the wavevectors, compute the specific heat of a cubic quantum dot with the following lengths: 10 Å, 20 Å, and compare it with the specific heat of the bulk crystal.

4.19 *Blackbody radiation in a small cavity.* Consider thermal radiation in equilibrium inside such a cubic cavity. Compute the radiation energy density in a cubic cavity of length $L = 1$ μm at $T = 400$ K and compare it with the Planck distribution obtained by assuming that the cavity is very large compared to the wavelength.

4.20 *Entropy of one phonon state.* From eqs. (4.14) and (4.40), show that the entropy, s, of one phonon state having a frequency ω obeys the following relationship:

$$\frac{\hbar\omega}{T} f_0(1 + f_0) = -\frac{\kappa_B T}{\hbar} \frac{\partial s}{\partial \omega}$$

Where f_0 is the Bose–Einstein distribution.

5

Energy Transfer by Waves

The wave–particle duality of matter from quantum mechanics implies that energy carriers have both wave and particle characteristics. One way to think about this duality is that material waves are granular rather than continuous. For example, a phonon wave at frequency ν contains a discrete number of identical waves, each having an energy $h\nu$. A fundamental property of waves is their phase information. A coherent wave has a fixed relationship between two points in space or at two different times. Due to the fixed phase relationship, the superposition of waves from the same source creates interference and diffraction phenomena that are familiar in optics.

The wave characteristics of matter (electrons, phonons, and photons) are important for transport processes at interfaces and in nanostructures. We have seen in previous chapters that the size effects on energy quantization can be considered as a result of the formation of standing waves. In this chapter, we will discuss the reflection of waves at a single interface, and interference and tunneling phenomena in thin films and multilayers. We will make parallel presentations for three major energy carriers: electrons, photons, and phonons. We have discussed rather extensively in chapters 2 and 3 the electron waves based on the Schrödinger equation. Optical wave effects are readily observable and can be understood from classical electrodynamics based on the Maxwell equations, which will be reviewed in this chapter. For phonons, we will adapt a continuum approach based on the acoustic waves, rather than on the discrete lattice dynamics method we used in chapter 3. The acoustic-wave-based approach allows us to treat phonons in parallel with electrons and photons. We will see that wave reflection, interference, and tunneling phenomena can occur for all three types of carriers and the descriptions of these phenomena are also similar (table 1.4), despite the differences in their statistical behavior, dispersion, and origin (table 1.3), as we discussed in previous

chapters. Readers familiar with any of these waves can use the analogy for understanding the other waves.

For macroscale transport processes, however, we seldom consider the phase of material waves. Rather, we treat the entities as particles. Why and when can we do so? Section 5.6 answers these questions and briefly discusses transport in the partially coherent regime.

5.1 Plane Waves

When throwing a stone into water, one can observe a concentric wave propagating outward. Television antennas emit electromagnetic waves that are approximately spherical. Rather than considering these nonplanar waves, we will carry out most of our discussion in this chapter on the basis of plane waves, although the phenomena to be discussed also exist for other forms of waves such as the cylindrical or spherical waves. A *plane wave* is one that has a constant amplitude at any plane perpendicular to the direction of propagation at any fixed time. These waves must satisfy the equation governing their motion. Later, we will discuss these governing equations, such as the Maxwell equations for electromagnetic waves. Before getting into these details, let's first examine some common forms of plane waves. For example, in chapter 2, we showed that the wavefunction of a free electron is [eq. (2.34)]

$$\Psi(x,t) = A_1 e^{-i(\omega t - kx)} + A_2 e^{-i(\omega t + kx)} \tag{5.1}$$

where the first term represents a plane wave traveling in the positive x-direction and the second term in the negative x-direction. These are scalar plane waves because the wavefunction is a scalar. Other waves, such as the electromagnetic field, are vector waves because the electric/magnetic fields have directions. We can express a harmonic, vector plane wave propagating in three-dimensional space as

$$\mathbf{F}(t,\mathbf{r}) = \mathbf{A}\sin(\omega t - \mathbf{k}\bullet\mathbf{r}) \tag{5.2}$$

where $\mathbf{A}$ represents the amplitude and direction of the field (e.g., electric, magnetic, or atomic displacement), ω is the angular frequency, $\mathbf{k}$ [with components (k_x, k_y, k_z)] is the wavevector representing the direction of wave propagation and its spatial periodicity ($|\mathbf{k}| = 2\pi/\lambda$), and $\mathbf{r}$ is the spatial coordinate. Equation (5.2) is a plane wave because all the points $\mathbf{r}$ satisfying $\mathbf{k}\bullet\mathbf{r} = constant$ form a plane perpendicular to the wavevector $\mathbf{k}$, and the field $\mathbf{F}$ is a constant on this plane at any given time.

Very often, it is much more convenient to use the complex representation rather than the sine and cosine representation for the waves. For example, instead of eq. (5.2), we can write $\mathbf{F}$ as

$$\mathbf{F}(t,\mathbf{r}) = \mathbf{A}\exp[-i(\omega t - \mathbf{k}\bullet\mathbf{r})] \tag{5.3}$$

When using such a complex representation, we resort to either the real part or the imaginary part of the final solution as the solution of the problem, in accordance with whether the initial or boundary conditions are represented in terms of cosine (real part) or sine (imaginary part) functions. For example, the imaginary part of $\mathbf{F}$ in eq. (5.3) is

identical to eq. (5.2) and we thus expect that the solution to a physical problem will be the imaginary part of the complex variables used in solving the governing equations.

In the following sections, we will examine three types of waves: the electron wave as a material waves, the electromagnetic wave governing the radiation transfer, and the acoustic wave representing lattice vibration.

5.1.1 Plane Electron Waves

In chapter 2, we dealt extensively with electron waves in planar geometries, such as free electrons and electrons in a potential well. The wavefunction of a plane electron wave propagating along the positive x-direction is

$$\Psi(x,t) = A\exp[-i(\omega t - kx)] \tag{5.4}$$

From the Schrödinger equation, we obtained in chapter 2 the following dispersion relation between the electron energy E and wavevector k

$$k = \sqrt{\frac{2m(E-U)}{\hbar^2}} \tag{5.5}$$

where U is the electrostatic potential. The particle current (or flux) can be calculated from [eq. (2.31)]:

$$\mathbf{J} = \frac{i\hbar}{2m}(\Psi\nabla\Psi^* - \Psi^*\nabla\Psi) = \mathrm{Re}\left[\frac{i\hbar}{m}\Psi\nabla\Psi^*\right] \tag{5.6}$$

As we will see later, this flux expression is similar to the Poynting vector that represents the energy flux of electromagnetic and acoustic waves.

5.1.2 Plane Electromagnetic Waves

In this section, we will introduce the Maxwell equations that govern the propagation of electromagnetic waves. We will show that a plane wave of the form of eq. (5.3) satisfies the Maxwell equations and discuss how to calculate the energy flux of the electromagnetic waves.

An electromagnetic wave in vacuum is characterized by an *electric field vector* $\mathbf{E}$ [$\mathrm{N\,C^{-1}} = \mathrm{V\,m^{-1}}$], and a *magnetic field vector* $\mathbf{H}$ [$\mathrm{C\,m^{-1}\,s^{-1}} = \mathrm{A\,m^{-1}}$]. When the electromagnetic field interacts with a medium, under the force of the electric and magnetic fields the electrons and ions of the atoms in the medium are set into motion. These electrons and ions generate their own electric and magnetic fields that influence each other and are superimposed onto the external fields. For example, the positive ions and negative electrons of an atom under an external field will be deformed from the original equilibrium condition, forming an electrical dipole.* A measure of the capability of the material to respond to the incoming electric field is the electric polarization per unit

*A dipole is a pair of positive charge Q and negative charge $-Q$, separated by a small distance a. The dipole moment of the pair of charges equals $p = Qa$.